Magnetic Resonance Studies of Hierarchically Ordered Replicas of Wood Cellular Structures Prepared by Surfactant-Mediated Mineralization

Li-Qiong Wang,* Yongsoon Shin, W. D. Samuels, and Gregory J. Exarhos

Material Science Department, Pacific Northwest National Laboratory, Richland, Washington 99352

I. L. Moudrakovski,* V. V. Terskikh, and J. A. Ripmeester

Steacie Institute for Molecular Sciences, National Research Council, Ottawa, Ontario, Canada K1A 0R6

Received: January 9, 2003; In Final Form: June 23, 2003

Hierarchically ordered positive and negative replicas of wood cellular structures prepared using surfactant templating methods under acidic and basic conditions have been studied by means of continuous flow hyperpolarized ^{129}Xe NMR, solid-state MAS ^{13}C, ^{29}Si, and 2D WISE NMR spectroscopic techniques. ^{129}Xe NMR data confirm a highly ordered and uniform structure with interconnected porosity in the positive silica wood replicas (SWR(+)) prepared under acidic conditions. In contrast, nonuniform porosity with irregular pore structures is inferred from similar data for negative silica wood replicas (SWR(−)) prepared under basic conditions. This contrasts with results from N_2 adsorption and TEM measurements that indicate regular nanoporous channels in both cases. From ^{13}C MAS NMR spectra, significant leaching of wood lignin was found to occur under acidic but was not evident for samples subjected to basic treatment. ^{29}Si MAS NMR spectra revealed higher hydroxylation levels for the silica replica prepared under acidic conditions compared to those observed in samples prepared under basic conditions. 2D WISE NMR experiments showed increased mobility of protons associated with the organic functional groups in cellulose after acidic treatment when compared with the dry and base-treated wood. Reported NMR data provide compelling evidence for the proposed mechanism of surfactant directed mineralization of wood cellular structures in acidic and basic solutions.

Introduction

Biological systems, even primitive ones such as diatoms, comprised chiefly of amorphous silica, exhibit architectures with highly ordered hierarchical organization.[1−3] Considerable efforts have been devoted to develop synthetic materials with multi-scale structural ordering similar to that found in natural materials.[4−18] Because these materials with an order from the nano- to the macro-scale have the advantage of multiple pore-size regions, they are excellent candidates for many technologically important applications including catalysis, selective adsorption, separation, mass-transportation, bioengineering, and environmental remediation.

Wood is a natural composite material and is comprised chemically of cellulose, hemicelluloses, and lignin. Microscopically, wood tissues contain interconnected cells (tracheas) and open spaces (lumens) and can exist in a wide variety of stable structures. They can be used as templates for the synthesis of inorganic materials where both structural and morphological complexities are required. Despite major efforts directed at simulating such structures,[14−18] only a few research groups have been able to synthesize positive wood replicas with multi-scale ordering. In a recent communication,[18] we have reported the synthesis of hierarchically ordered ceramics produced by in situ mineralization of wood cellular structures using a low pH surfactant-templated sol−gel processing method. Hierarchically ordered architectures prepared by this method not only reproduce the cellular structures of the biological tissue but they also harbor organized nanoporous channels within the cell walls. This approach allows reproduction of the cellular structures in great detail. The entire mineralized wood sample, including interconnected cells, pit structures, multilayered cell walls, and oriented fibrous features, was well preserved even after all of the organic contents had been removed by heating. These hierarchical porous materials with high surface area (up to 650 m^2/g) have potential for the immobilization and stabilization of large biomolecules and agents and are of considerable interest as they allow enhanced mass transport and faster reaction kinetics.[18] More recently, a zeolite-based reproduction of wood cellular structure has also been reported.[17] As yet, little effort has been devoted to the investigation of the formation mechanism of materials with both ordered nano- and macro-porosities. It is important to investigate the pore structure and the formation mechanism at a molecular level in order to develop rational design strategies for producing novel materials with tailored multidimensional pore structures. Although nanoporosity and wood cellular macro-structures have been observed previously with TEM and SEM,[17,18] the detailed pore structure in such material remains unknown. In addition, it is not clear how solution pH controls the formation of positive (SWR(+)) or negative (SWR(−)) silica wood replicas in which all void spaces are clogged with precipitated ceramic precursors. Because the inorganic precursors also will likely interact with chemical functional groups intrinsic to the wood cellular structures, it is also crucial to examine the wood structure itself as it is treated

* To whom correspondence should be addressed. E-mail: lq.wang@pnl.gov (L.Q.W.); igor.moudrakovski@nrc.ca (I.L.M.).

10.1021/jp030027f CCC: $25.00
Published on Web 11/19/2003

under different pH conditions in order to understand the processes by which positive and negative replicas are formed.

Introduced about 20 years ago,[19,20] ^{129}Xe NMR spectroscopy of porous materials has become a popular technique for structural characterization; several extensive reviews on the subject are available.[21−23] However, the application of ^{129}Xe NMR to pore systems has concentrated mostly on crystalline porous materials such as zeolites; only a limited number of studies of either amorphous or highly disordered pore systems are available. Recently, we reported the first application of hyperpolarized ^{129}Xe in continuous flow to studies of ordered nanoporous materials.[24] As compared with X-ray powder diffraction measurements, transmission electron microscopy and nitrogen sorption, which in principle provide information on pore size, pore volume, and surface area, ^{129}Xe NMR spectroscopy has the advantage of probing the connectivity and the uniformity of the pores which are not accessible by other techniques. The use of optical pumping techniques for the production of hyperpolarized (HP) xenon allows an increase in sensitivity of several orders of magnitude.[25] Because this technique works at very low concentrations of xenon, the contribution of Xe−Xe interactions within the porosity is negligible and the observed ^{129}Xe chemical shifts can be assigned mainly to interactions between the xenon atoms and the surface. Variable temperature measurements provide additional information on the adsorption parameters of xenon and, for the nanoporous materials studied, reveal a nonuniform porosity and irregular pore structure in cases where N_2 adsorption and TEM indicate regular nanoporous channels.[24]

Comparative ^{129}Xe NMR studies of pore structures and connectivity in positive and negative replicas prepared under acidic and basic conditions are helpful for the understanding of the formation mechanism of such materials. Complementary information on the structural organization of the framework, its crystallinity, and conformational ordering of the organic template can be obtained from solid-state ^{29}Si NMR[26−31] and ^{13}C NMR[26,30,32] spectroscopy. ^{13}C MAS NMR spectra can be used to monitor the changes in wood structure after solution processing, whereas ^{29}Si NMR can be used to examine the hydroxylation and condensation of silica precursors under different pH conditions. The mobility and conformation of the flexible side chains in stiff macromolecules can be probed by two-dimensional wide-line separation (2D WISE) NMR spectroscopy as developed by Spiess and co-workers.[33,34] Because of the limited chemical shift range, one-dimensional ^{1}H NMR measurements alone are insufficient to distinguish the proton signals in different chemical environments in the solid state. In 2D WISE NMR, the proton line-widths associated with the individual carbon sites can be resolved by acquiring the ^{1}H spectrum in one dimension and the high-resolution ^{13}C CP MAS spectrum in the other dimension. In rigid crystalline solids, the strong dipolar interactions due to the abundant proton spins give rise to broad proton line-widths. However, the line-widths of the proton are significantly reduced in semicrystalline solids or liquid environments because of weaker dipolar interactions caused by increased molecular motion, indicating that the proton line-widths obtained from 2D WISE NMR are sensitive probes of the local chain dynamics. The mobility of the functional groups on the surface of the cellular structures before and after processing in acidic or basic solutions is assessed using 2D WISE NMR. Thus far, NMR studies on the chemical structure and dynamics of as-synthesized wood replicas with multiscale ordering have not been reported. The combined results of ^{129}Xe, ^{13}C, ^{29}Si, and ^{1}H 2-D WISE NMR measurements described here provide better insight into the mechanism of formation of silica replicas.

Experimental Section

Materials. Hierarchically ordered silicates were synthesized by an in situ mineralization of wood cellular structures with surfactant-templated sol−gel solutions at different pH. Poplar and pinewood were obtained from Eagle Hardware (Kennewick, WA) and used without further treatment. Tetraethyl orthosilicate (TEOS), sodium silicate (27.0 wt %), HCl, and EtOH were purchased from Aldrich Chemical Co., and cetyltrimethylammonium chloride (CTAC) was purchased from Kodak Co. Woods and reagents were used without further treatment or purification. The technique used for acid-catalyzed sol−gel mineralization appears in a previous report.[18] A relatively high volume ratio of EtOH to H_2O was used to prevent precipitation of silica from solution. The use of an acidic alcoholic solution also prevents the leaching of lignin from the wood network. In the basic system, 27.0% sodium silicate solution was used as a silicate precursor: SiO_2/CTAC/NaOH/H_2O = 1.0:0.5:2.0:120. Several samples of wood treated in the sol−gel solution were kept at 60 (acidic condition) or 40 °C (basic condition) for several days in a sealed polypropylene container. The wood samples were then removed from solution and immersed in a fresh solution for a several more days at the same temperature. After 3 cycles, the samples were removed from the sol mixture, air-dried, and calcined at 550 °C for 6 h.

Characterization of Physical Properties. The physical properties of samples prepared under acidic conditions have been described previously. Detailed results for samples prepared in both basic and acid conditions will be reported separately. To summarize, XRD patterns of as-synthesized SWR materials showed that the architecture of the wood cellular structures was preserved with little change after acid treatment. The surfactant-templated liquid-crystalline solution produced hexagonally ordered nanoporous silicate networks.[18] TEM images showed that the cell walls in calcined poplar samples prepared under either condition are hexagonally ordered with 20 Å diameter pores, whereas BET measurements of calcined samples prepared under either condition showed higher surface areas (up to 700 m^2/g) than for silica materials prepared without the surfactant ($\leq$50 m^2/g). SEM images of SWR materials following calcination show that these ordered samples retain their original cellular structures with positive or negative contrast at either low or high magnification. At low magnification, samples prepared at low pH show intact cells, cell walls, and pit structures in the cell walls. In addition, under high magnification, they show ray pitting of poplar, rectangular-type cells with fibrous arrays, and bordered pits for pine. In contrast, calcination of silica samples prepared at high pH leads to negative replicas. At low magnification, filled tube-type cells with negative images of pits were observed, and at high magnification, negative vessel pittings in the cell walls and negative bordered pits of a donut type were observed. To facilitate further discussion, an illustrative diagram of the formation of positive and negative silica replicas is shown in Scheme 1.

NMR Measurements. ^{129}Xe NMR experiments were performed on calcined silica replicas with hyperpolarized (HP) ^{129}Xe produced in a continuous flow (CF) apparatus described previously.[25,35] A 30 W diode laser (OptoPower Corporation) was used in this setup; the optical pumping cell was located in the fringe field of the spectrometer magnet. A xenon−helium−nitrogen mixture with a composition of 1%−98%−1% was used

SCHEME 1: Schematic Illustration of the Formation of Positive and Negative Silica/Wood Replicas: SWR(+) and SWR(−)[a]

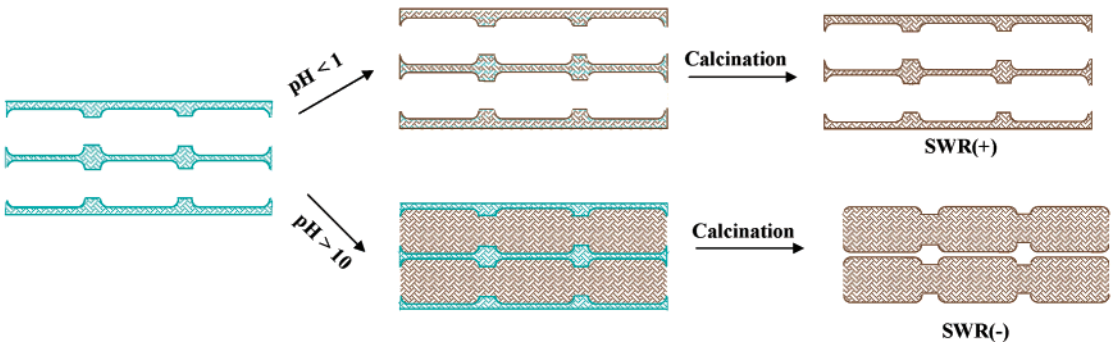

[a] Two cells with curved inner cell walls are shown on a length scale of 10−20 μm for the purpose of illustrating the different formation mechanisms under both basic and acidic conditions.

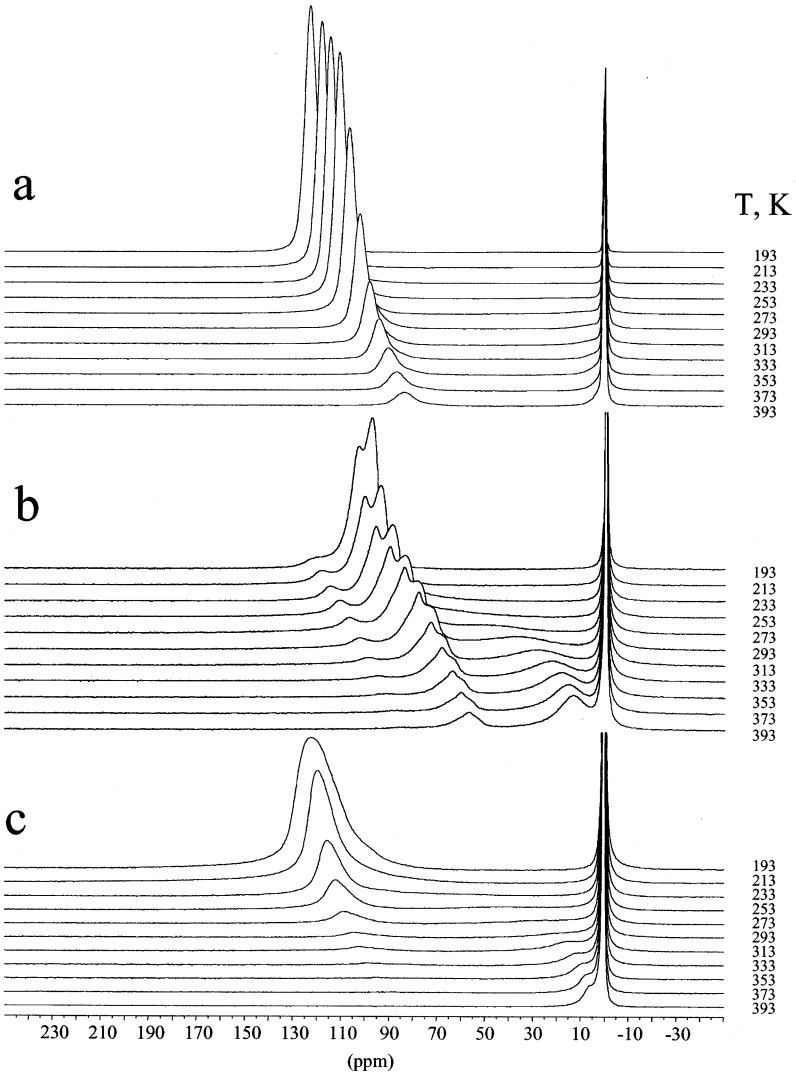

Figure 1. ^{129}Xe NMR spectra obtained at various temperatures with a continuous flow of hyperpolarized xenon adsorbed in samples of mineralized wood prepared by different procedures. (a) Poplar treated under acidic conditions, (b) Poplar treated under basic conditions, and (c) Poplar treated under neutral conditions.

in all experiments. The flow rate was monitored with a Vacuum General flow controller (model 80-4) and kept constant during the experiments in the range of 200−250 scc/min (scc/min, gas flow normalized to standard conditions). The probe used for continuous flow experiments was a modified static-sample probe obtained from Morris Instrument Inc., which allowed continuous delivery of the HP xenon−helium mixture directly into the coil region over the temperature range from 120 to 400 K. All ^{129}Xe NMR spectra were obtained on a Bruker DSX-400 spectrometer (magnetic field 9.4 T, ^{129}Xe resonance frequency 110.6 MHz). The reported ^{129}Xe NMR chemical shifts were referenced to xenon gas extrapolated to zero pressure.

Solid state ^{13}C and ^{29}Si MAS (magic angle spinning) NMR experiments were carried out with a Chemagnetics spectrometer

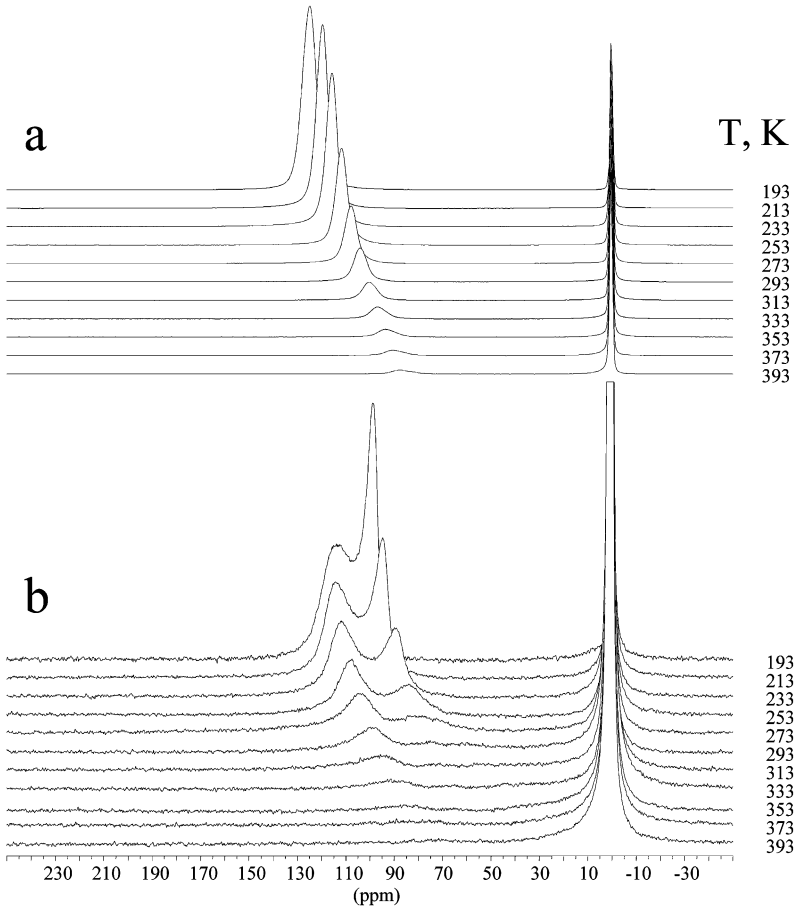

Figure 2. Variable temperature continuous flow ^{129}Xe NMR spectra of xenon adsorbed in samples of mineralized wood. (a) Pine treated under acidic conditions and (b) Pine treated under basic conditions.

(magnetic field 7.05 T, resonance frequencies 75.0 and 59.3 MHz, respectively) using a variable temperature double-resonance probe. For ^{13}C NMR experiments, both single-pulse (SP) Bloch-decay and cross-polarization (CP) methods were used with ^{1}H decoupling. Samples were loaded into 7-mm zirconia PENCIL rotors and spun at 3−4 kHz. SP spectra were collected with a 4.5 μs (90°) ^{13}C pulse, and a repetition delay of 10−60 s. The number of transients was 1000−3000. SP ^{29}Si MAS NMR spectra with ^{1}H decoupling were obtained for all samples spun at 3−4 kHz. Both ^{13}C and ^{29}Si NMR chemical shifts were referenced to tetramethylsilane at 0 ppm

Two-Dimensional Wide-Line Separation NMR Spectroscopy (WISE) with the Usual 2D WISE Pulse Sequence:[33] a ^{1}H 90° pulse is applied and this is followed by an incremented proton evolution period t_1. After each t_1 period, cross polarization (CP) pulses were followed by a TOSS (total suppression of spinning sidebands) sequence.[36] The subsequent carbon detection with proton decoupling gives a modulated ^{13}C spectrum as a function of t_1 because of the free induction decay of the associated protons. The two-dimensional Fourier transform gives a 2D spectrum with high-resolution ^{13}C CP MAS spectra in one dimension and the proton wide-line spectra associated with each carbon in the other dimension. In our measurements, a 90° pulse width for both ^{1}H and ^{13}C pulses was 4.5 μs. The ^{13}C CP MAS spectra were taken with a contact time of 0.15 ms and a pulse delay of 3 s. The 2D data size was 128 points in the t_1 (^{1}H) dimension and 1k in the t_2 (^{13}C) dimension. The spectral width in t_1 was 200 kHz (dwell time, 5 μs) and 20 kHz in t_2 (dwell time 50 μs). Amplitude spectra were used for the proton dimension (^{1}H).

Results

First, we present ^{129}Xe NMR results for calcined silica replicas of poplar and pinewood prepared under different pH conditions that provide information on connectivity and distribution of pores. For as-synthesized poplar/silica composites prepared under acidic or basic conditions, ^{13}C NMR measurements were used to examine structural changes in the wood during the mineralization process. ^{29}Si NMR results are used to monitor the connectivity of silica in wood/silica composites before and after calcination. Finally, 2D-Wise NMR spectra yield information on the dynamics of the C−H interactions in the wood cellular structures derived from the different precursor solutions.

^{129}Xe NMR. Figures 1 and 2 depict ^{129}Xe NMR spectra recorded as a function of temperature for the calcined silica replicas of poplar and pine prepared under acidic and basic conditions, respectively. The silica samples of both wood replicas prepared at low pH show rather narrow and relatively symmetric lines throughout the temperature range (Figures 1a and 2a). This demonstrates homogeneity of localized environments, a rather narrow distribution of mesopore sizes, and rapid exchange among different pore spaces. Table 1 summarizes room temperature ^{129}Xe chemical shifts and corresponding mean pore diameters as derived according to the ref 37. In a general agreement with TEM data, our ^{129}Xe results indicate for all mineralized samples a presence of pores in a range of 1.3−2.1 nm in diameter. For pine and poplar samples mineralized in basic conditions, ^{129}Xe NMR spectra show some additional more shielded signals corresponding to larger pores between 5 and 7 nm in diameter.

TABLE 1: Room Temperature ^{129}Xe NMR Chemical Shifts for SWR Samples and Corresponding Mean Pore Diameters Calculated According to Ref 37

sample	media	δ (^{129}Xe, 293 K), (±0.5) ppm	D, (±0.2) nm
poplar	acidic	102.3	1.6
	basic	72.0	7.2
		78.3 (main signal)	5.6
		102.8	1.5
	neutral	104.7	1.3
pine	acidic	104.0	1.4
	basic	101.8	1.6
		73.8	6.7
		98.7 (main signal)	2.1

The line intensity decreases dramatically with increased temperature because of reduced adsorption of Xe at higher temperature. The line width, however, remains relatively narrow, indicative of fast exchange. Overall, the spectra of poplar mineralized under acidic conditions are very similar to those for the pine sample. Only small differences can be seen in the rate of change of the chemical shift with temperature. The variable temperature dependence of the chemical shifts in the CF HP ^{129}Xe NMR experiments is summarized in Figure 3. Assuming only weak adsorption of xenon, as described by Henry's law, one can extract quantitative information on the Xe adsorption. In the fast exchange approximation the temperature dependence of the observed chemical shift δ for cylindrical pores can be expressed as[24,37]

$$\delta = \delta_s\left(1 + \frac{D}{4K_0RT^{1/2}\exp\left(\frac{\Delta H_{ads}}{RT}\right)}\right)^{-1} \quad (1)$$

where D is the pore diameter, K_0 is the pre-exponent in Henry's equation, R is the universal gas constant, ΔH_{ads} is the heat of adsorption, and δ_s is the ^{129}Xe chemical shift characteristic of the surface. By fitting the temperature-dependent data given in Figure 3 with the above function,[24,37] one can estimate the heats of adsorption for xenon at 8.5 ± 0.7 and 9.3 ± 0.9 kJ/mol for mineralized pine and poplar, respectively, which indicates very weak and unrestricted physical adsorption.

The ^{129}Xe NMR spectra for the sample of poplar mineralized under neutral conditions (Figure 1c) are somewhat similar to the sample prepared under acidic conditions; however, they are noticeably broader at all of the temperatures. At a higher temperature, the line broadens to such an extent that it disappears almost completely. At the same time, an additional line emerges at a chemical shift between 20 and 0 ppm. Such signals often are observed when very small particles of adsorbent are present and normally are assigned to xenon adsorbed on external surfaces of the particles. Overall, the spectra indicate that the porous environment in the sample prepared under neutral conditions is not as ordered as that seen for samples prepared in acidic media. The heat of adsorption for xenon determined from fitting the $\delta(T)$ dependence (Figure 3c), 10.0 ±1.1 kJ/mol, is similar to that observed for mineralized poplar prepared in acidic media.

The many lines observed in the ^{129}Xe NMR spectra for samples prepared in basic media (Figures 1 b and 2b) are the result of inhomogeneities and rather broad distributions in the size of the pores with a reduced rate of xenon exchange between different adsorption regions. It appears that mineralization of both pine and poplar in basic media leads to considerably less homogeneous porosity than in the case of samples treated in low pH solutions. The heats of adsorption for xenon determined from the fitting of the $\delta(T)$ dependencies (Figure 3b) are 11.0 ±1.4 kJ/mol for poplar and 15.4 ±1.2 kJ/mol for pine (only one line in each spectrum that is observable throughout all of the range of the temperatures has been used in the fitting).

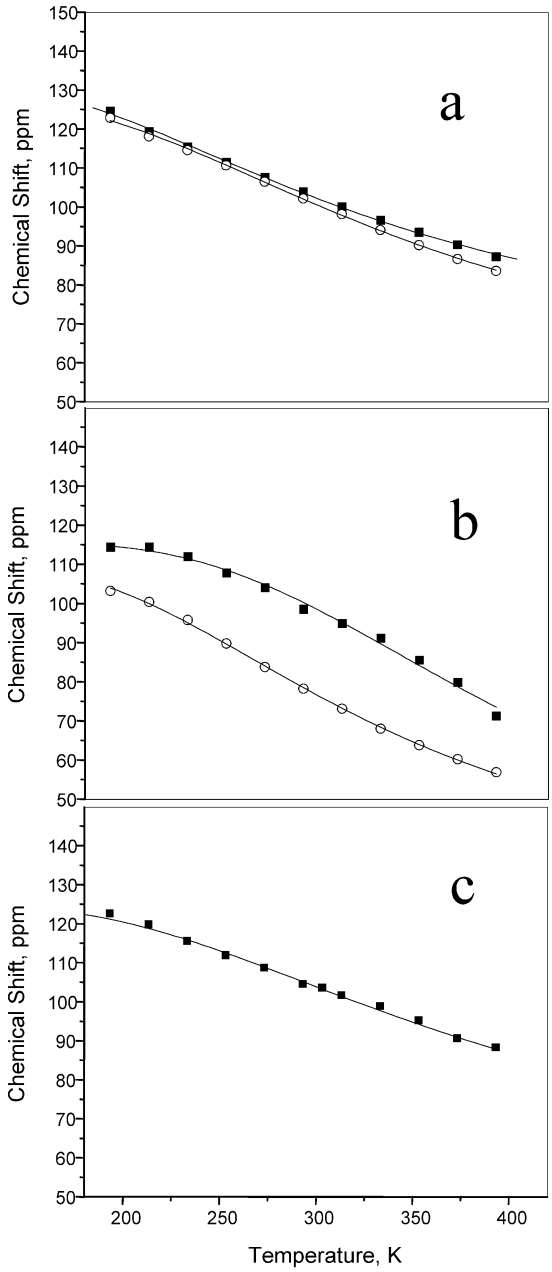

Figure 3. Temperature dependence of the ^{129}Xe chemical shift of xenon adsorbed in mineralized wood. Continuous lines are fits of the experimental points with eq 1 in the text. (a) Acidic preparation: solid blocks, pine; open circles, poplar; (b) Basic preparation: solid blocks, pine; open circles, poplar; (c) Neutral preparation, poplar.

The heat of Xe adsorption in the sample of poplar is similar to that in samples prepared by acidic and neutral treatments, whereas for pine, the value is almost twice as high. This increase may relate to a higher microporosity in the pine sample, though we need to note that the smaller pore size is not always associated with the higher heat of adsorption. A somewhat higher value of the chemical shift for xenon on the surface (limiting value of δ at low temperatures) for the pine sample can also be an indication of higher microporosity.

^{13}C and ^{29}Si NMR. ^{13}C CP MAS NMR spectra of untreated poplar and poplar/silica composites prepared in basic and acidic

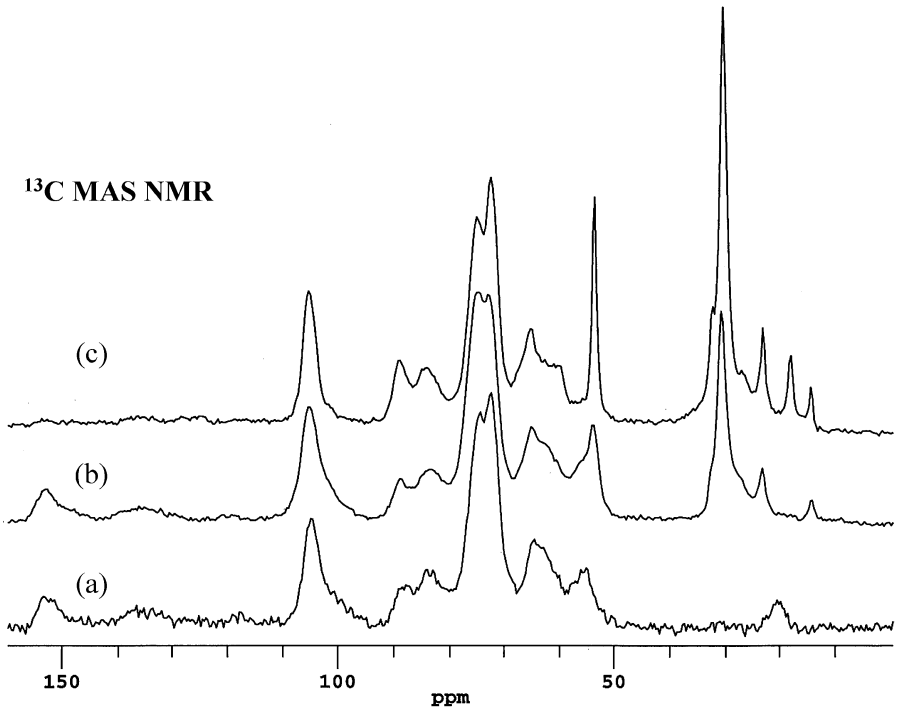

Figure 4. 4CP-MAS ^{13}C NMR spectra of (a) untreated poplar wood and as synthesized poplar/silica composites prepared in (b) basic and (c) acidic solutions. The signal at 18 ppm in Figure 4c is due to the small amount of residual ethanol used as a solvent.

media are shown in Figure 4. Based on the values reported previously for the untreated poplar,[38−40] we assign the signals ranging from 50 to 110 ppm to cellulose carbon, the signal at 153 ppm to phenolic carbon in lignin, and the signal at 22 ppm to the methyl group of hemicelluloses (Figure 4a). The ^{13}C NMR spectrum shown in Figure 4b for the poplar/wood composite prepared in basic solution resembles that for the untreated poplar wood, indicating the wood structure to be intact for the poplar wood after mineralization under basic conditions. Additional relatively sharp features in the chemical shift region from 14 to 35 ppm are attributed to the surfactant CTAC used in the templated mineralization process. The single dominant resonance at ~31 ppm in both parts b and c in Figure 4 is associated with the internal methylenes (C4−14) of the surfactant molecules in amorphous silica.[32] However, after mineralization under acidic conditions, the poplar wood shows a somewhat different spectrum (Figure 4c). Disappearance of the signal at 153 ppm (associated with lignin) suggests that this component of poplar wood was leached away by the acid treatment. The features corresponding to the CTAC surfactant are more pronounced in Figure 4c than in Figure 4b. The sharp, intense feature at 54 ppm in Figure 4c is also associated with CTAC, which partially overlaps the cellulose signal.

^{29}Si MAS NMR spectra for the as-synthesized poplar/silica composites, prepared under acidic and basic conditions, are given in Figure 5. In general, ^{29}Si resonances at approximately −90, −100, and −109 ppm are assigned to Q^2, Q^3, and Q^4 units, respectively, where Q^n is $SiO_n(OH)_{(4-n)}$.[41] The degree of polymerization of the silica framework is proportional to the relative amount of Q^4 species. Three well-resolved relatively narrow resonances at −91 (Q^2), −101 (Q^3), and −109 ppm (Q^4) are observed in Figure 5b for the poplar wood treated in acidic media, whereas the poplar wood prepared under basic conditions gives three less well resolved, broader resonances at −90 (Q^2), −99 (Q^3), and −108 ppm (Q^4) (Figure 5a). The spectrum in Figure 5 exhibits a larger Q^3/Q^4 ratio of 2.4 for the as-synthesized poplar/silicate composite derived from acidic media

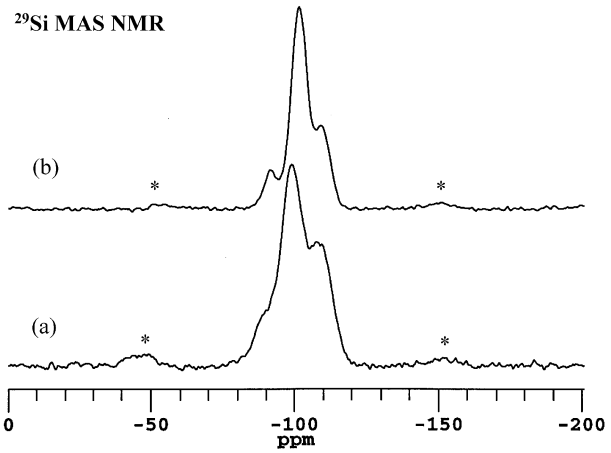

Figure 5. Single-pulse MAS ^{29}Si NMR spectra of as synthesized poplar−silica composites prepared in (a) basic and (b) acidic solutions. The asterisk (*) indicates spinning sidebands.

than that of 1.1 from basic media. Because both samples have a similar surface area, the higher Q^3/Q^4 ratio indicates a higher degree of hydroxylation for the silica in the wood replica from acidic media than that from basic media.

2D WISE Measurement. Figure 6 shows 2D WISE NMR spectra for the untreated poplar and calcined poplar/silica composites prepared in acidic and basic media, and their corresponding slices in the ^1H dimension for the cellulose carbons at 73 ppm (the most intense resonance in ^{13}C NMR spectra in Figure 4) are given in Figure 7. The chemical shift range in the ^{13}C dimension in Figure 6 was plotted from 60 to 160 ppm in order to emphasize the signals from cellulose rather than those from CTAC. 2D WISE NMR spectroscopy is used here to examine the changes in mobility of the cellulose component groups in poplar treated under different pH conditions. Because in diamagnetic solids proton line-widths determined from 2D WISE NMR measurements are determined by

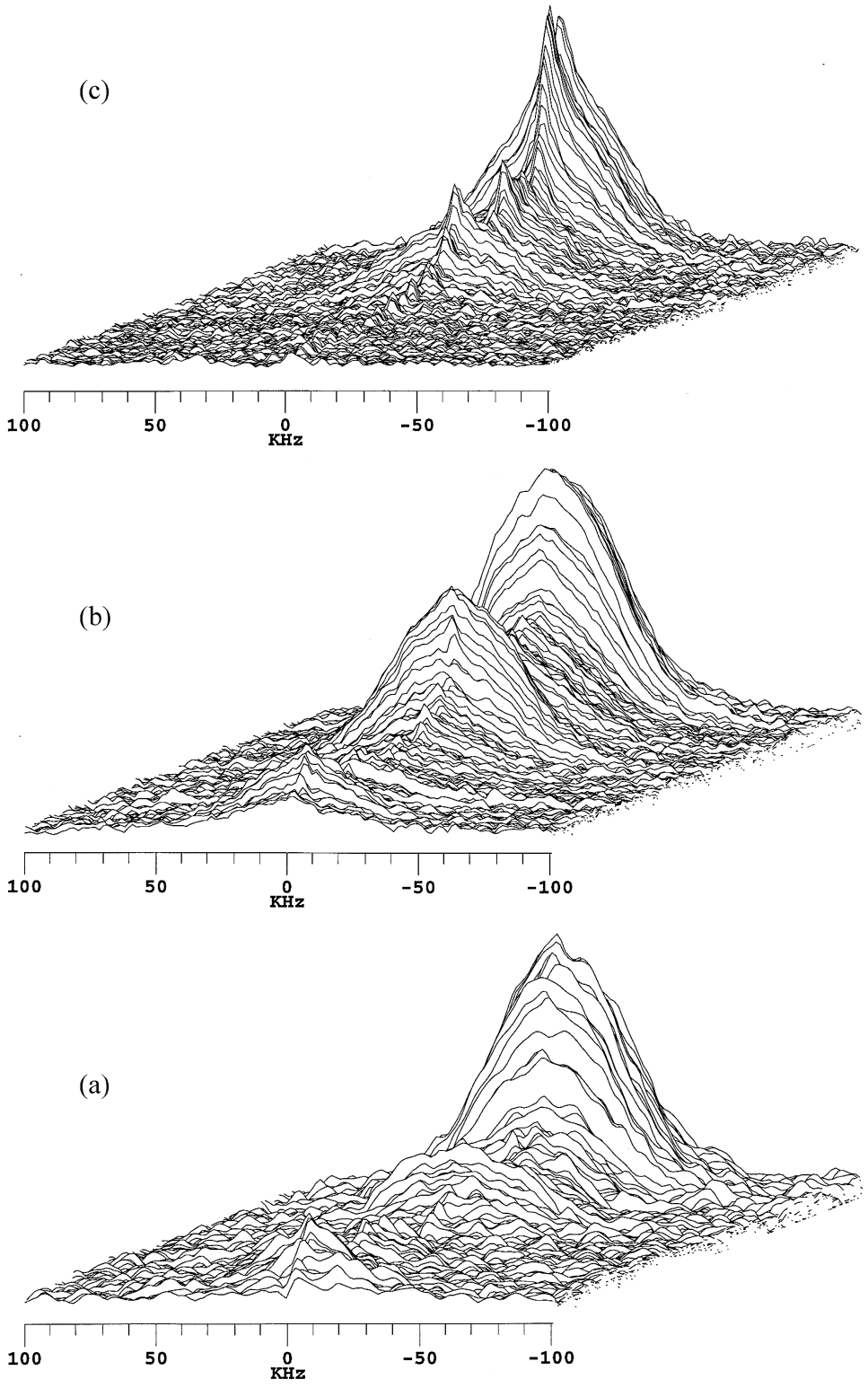

Figure 6. 2D WISE NMR spectra for (a) untreated poplar, and poplar/silica composites prepared under (b) basic and (c) acidic conditions. The horizontal axis is the ^{1}H dimension.

the dipolar couplings among the ^{1}H spins, they are also sensitive to the mobility of the specific proton-bearing carbon groups. In solids containing mainly rigid methylene groups, line widths typically range from 50 to 70 kHz. These proton line widths are significantly smaller in the presence of sufficiently rapid molecular motion that averages the dipolar interactions.

The overall features in the 2D WISE NMR plot for poplar/silica prepared under basic conditions (Figure 6b) resemble those for the untreated poplar wood (Figure 6a) but clearly differ from the spectra of poplar/silica prepared under acidic conditions (Figure 6c). Both untreated poplar and poplar treated in basic media show similar broad 1D ^{1}H spectra with fwhm values of 62 and 58 kHz, respectively (Figure 7). However, the 1D ^{1}H spectrum for the acid treated poplar (Figure 7c) is likely a superposition of a narrow (fwhm of 10 kHz) and a broad component, with the broader component of about the same width

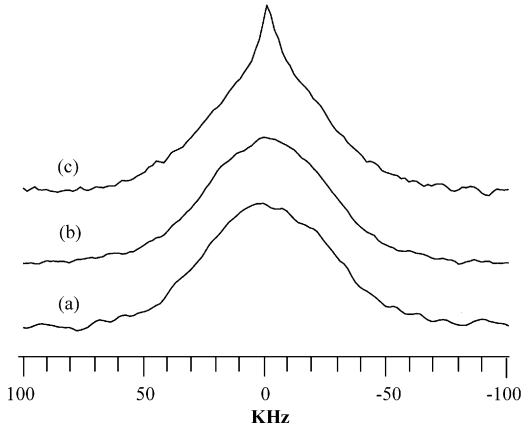

Figure 7. Slices of Figure 6 in the ^{1}H dimension at 73 ppm of the wood cellulose ^{13}C resonance (the most intense signal in ^{13}C NMR spectra of Figure 4). (a) Untreated poplar, (b) poplar/silica composites prepared under basic conditions, (c) Poplar/silica composites prepared under acidic conditions.

as in the spectra shown on Figure 7b (the ratio of narrow to broad components is about 1:10). The small narrow component observed in Figure 7c suggests an increased mobility of cellulose carbon groups at 73 ppm in the acid treated poplar. The line width of 62 kHz for the untreated wood is in the range for rigid solids, indicating immobile crystalline cellulose. Similar line widths for the cellulose protons observed for the untreated poplar and treated poplar in basic media suggest that undisturbed crystalline cellulose survives upon treatment at high pH.

Discussion

Scheme 1 gives a simplified graphic illustration for two different mechanisms for the sol−gel syntheses of SWR(+) and SWR(−) materials. This simplified picture shows two wood cells with curved inner cellular walls on the length scale of 10−20 μm. In fact, wood has a very complex architecture consisting of interconnected cells (tracheas) and open spaces (lumens). The cell walls usually contain a thin layer called the primary wall and a thicker layer called the secondary wall. Theses cells are glued together by an intercellular layer (or middle lamella) and are connected by openings of different shapes. These openings are called pits (bordered or simple pits) and serve as communication channels between cells.

When a positive replica is prepared under acidic conditions (pH $\leq$ 0.1), silica precursors penetrate into the curved inner surfaces of the wood cellular structure and intercalate the cell wall. At the same time, the surfactant micellar structures insert into the silica network, which produces organized nanoporous channels during calcination. At low pH, most of the silica precursor (TEOS) is hydrolyzed and condensation proceeds slowly.[42] The slow condensation under acidic conditions allows silica precursors enough time to penetrate into the poplar wood cellular structure before precipitating from solution. The polar groups such as hydroxyl, carboxylic, and ester groups in the cellulose molecular structures most likely act as high affinity sites for the silicate condensation. This kind of in situ intercalation and mineralization during the synthesis of positive replicas under acidic conditions contrasts with the formation mechanism of the negative replica under basic conditions (pH $\geq$ 10). Instead of slow intercalation and mineralization, the negative replicas are formed as a result of fast condensation of the silica precursors at high pH followed by deposition of silica into the void spaces of the cells. In addition to the slow condensation kinetics of the silica precursor, which contributes to the formation of the positive replica under acidic conditions, significant leaching of lignin in poplar wood under acidic conditions is also a critical step in the formation of positive replica of the structure. Because lignin is an important constituent of the cell wall in all vascular plants,[43] leaching of lignin leads to continuous porous channels that provide pathways for the silicate species to penetrate into the wood cellular structure. This effect, however, is absent under basic conditions. Previous attempts to silicify[44,45] or to carbonize[46] wood tissues also produced small segments of the negative replica of wood structure in porous ceramic formed through the deposition of a ceramic phase within the wood interstices or infiltration of the ceramic into the unoccupied void space. Those materials, however, did not reproduce the structural nuances intrinsic to natural wood and are different from the negative replicas prepared in this study where the surfactant templated synthesis produces both macroscopically and mesoscopically ordered ceramics.

Our ^{129}Xe, ^{13}C, ^{29}Si, and 2D WISE NMR experiments support the proposed mechanisms. ^{13}C MAS NMR spectra (Figure 4) clearly show the removal of lignin from wood prepared under acidic conditions, whereas intact structures were observed for wood treated under basic conditions. More rapid hydrolysis and slower condensation of the silica precursors prepared in acidic rather than in basic media are seen in ^{29}Si MAS NMR spectra (Figure 5) where a higher Q^3/Q^4 ratio was found for the poplar/silica prepared in acidic media. The removal of lignin and slow condensation in acidic media allow silica precursors to penetrate into the inner surface of the cell structure in wood. The 2D WISE NMR experiment shows that some protons associated with organic functional groups in cellulose have indeed become more mobile as compared to the dry or base-treated wood. The more mobile cellulose groups associated with these protons most likely are those in close proximity to the lignin. Because lignin is one of the constituents which keeps the individual cells together, its removal upon acid treatment results in increased mobility for the nearby cellulose groups.

^{129}Xe NMR spectra clearly indicate the difference in structure and connectivity of the pores for the poplar/silica prepared under acidic and basic conditions. The variation in structure and connectivity of the pores is attributed to the different mechanisms for the formation of positive and negative replicas at different solution pH. Under acidic conditions, the silica precursors are hydrolyzed and condensed onto the cell wall leaving the majority of the void spaces and pits unoccupied, thus resulting in the formation of a positive replica (Scheme 1). In contrast, because of rapid condensation under basic conditions, the silica precursors clog the cells and pit structures, shutting off the communication channels between cells. Upon calcination, the wood/silica composites form positive wood replicas that reproduce accurately the wood cell structure with all of the extended pore interconnectivity. This highly ordered structure with connected channels gives rise to narrow and symmetric peaks measured in ^{129}Xe NMR spectra throughout the entire temperature region studied (Figure 1). ^{129}Xe NMR data for the silica replica prepared under acidic conditions suggest a high degree of homogeneity of the local environment, a narrow distribution of mesopores, and rapid exchange between regions of varying porosity. This is in contrast to the resident inhomogeneity and the broad distribution in pore sizes for the silica replica prepared in basic media. In materials produced under basic conditions^{129}Xe NMR peaks do not collapse even at elevated temperatures, likely indicating that the inhomogeneity is present not within the same sample region but rather in well-

separated regions that have pores of different sizes. These different sample regions are made of disconnected cells because the communication channels between cells are clogged in high pH processing solutions.

Although TEM micrographs show hexagonally ordered 20 Å pores for both silica samples of positive and negative replicas, ^{129}Xe NMR data clearly provides a more complex picture. Similar to TEM, the ^{129}Xe NMR results indicate pores of similar sizes for all samples (see Table 1). However, because the length scale of ^{129}Xe NMR is significantly large than TEM, μm as opposed to nm, it provides some complementary results to the TEM information. On another hand, the effective length on the order of microns is about the size of a single wood cell (5−100 μm), and the seeming differences between ^{129}Xe NMR data for different samples should be viewed mostly as differences in the larger, cell-size voids.

In a case of nonrestricted diffusion of Xe inside and between the cells (as thought in positive wood replicas, when only cellular walls are mineralized leaving intracell space empty and pits open), the adsorbed Xe atoms sample only cell walls, and its NMR line is narrow due to the fast exchange. The Xe NMR shift in this case would depend on the average size of nanopores in the sample. For a wide range of silica-based materials, we have found that there is a good quantitative correlation between these two parameters.[37] Comparing the pore sizes derived from NMR (Table 1) and TEM (and also adsorption data) for woods treated in acidic conditions (positive replicas), one can see a reasonably good agreement. This fact, together with narrow NMR lines, is an indication of homogeneous pore structure (of the cell walls) throughout the sample and unrestricted Xe diffusion (though the fact of observation of narrow NMR lines cannot exclude multimodal pore size distributions or heterogeneity on a molecular scale). When, however, the internal cell voids and connecting pits are getting clogged with silica (as in negative wood replicas as seen in SEM), multiple Xe NMR lines are observed due to different environments experienced by Xe atoms. Slow or no Xe exchange between these regions (^{129}Xe 2D EXSY data for similar systems to be published) and width of the lines (inhomogeneous broadening) both indicate an inhomogeneous structure of the material on the micrometers scale (about the cell size) with highly limited Xe exchange between different regions. In this respect, ^{129}Xe NMR spectra for the silica replica prepared under acidic conditions show a more uniform porosity than that for the silica replica prepared under basic conditions. This conclusion is also supported by SEM observations on the specific morphology of the negative wood replicas.[18]

Every experimental technique has its limitation, and it is not totally unexpected that TEM, XRD, and (in many cases) standard porosimetry fail to provide a rather important information about structural differences that potentially affect diffusion, adsorption, separation and catalytic properties of materials. TEM images can be not very representative due to a very small covered area. XRD patterns are characteristic only to highly ordered (in our case, nanoporous) regions of the sample. Nitrogen porosimetry is not very sensitive to larger voids and their connectivity when many smaller (nano-) pores are present. In such a situation, Xe appears to be a good additional probe for testing the hierarchy of the porous spaces.

As compared with the previous ^{129}Xe NMR data for ordered nanoporous silica,[24] ^{129}Xe NMR spectra in this study show narrower and more symmetric peaks at all temperatures. In part, this is because of the sol−gel mineralization process where the wood cell structure assists the formation of continuous porous channels and ordered nanopores. The slower kinetics for condensation of the silica may also contribute to a more ordered nanoporosity. Furthermore, the formation of connected channels as a result of the removal of lignin in acidic media is critical in maintaining structural integrity because interconnected pathways are available for the decomposed organics to leave without degrading the entire structure. This explains the fact that the mineralized wood samples prepared under acidic conditions retain their original shape after calcination and show higher mechanical integrity than the calcined samples prepared under basic conditions.

Conclusions

In this paper, we report a detailed multinuclear magnetic resonance study of hierarchically ordered positive and negative replicas of wood cell structures prepared by a templated mineralization method. ^{129}Xe NMR spectra show ordered and connected pores in wood replicas prepared in acidic media, whereas nonuniform pore distributions and poorer connectivity are found for wood replicas prepared under basic conditions. Significant leaching of lignin in acid treated wood was observed in the ^{13}C MAS NMR spectra. Removal of the lignin in wood creates pathways for silica precursors to penetrate into the cell network and to maintain the structural integrity upon calcination. ^{29}Si MAS NMR data revealed higher hydroxylation for silica replicas prepared under acidic conditions as compared to those prepared under basic conditions. 2D WISE NMR measurements indicate a higher mobility of a portion of the cellulose groups in the acid treated poplar mainly due to the removal of lignin. All NMR results consistently support the templated mineralization mechanism discussed in this study.

Acknowledgment. This work has been supported by the Division of Materials Sciences and Engineering, Office of Basic Energy Sciences U.S. Department of Energy (USDOE). The research described in this paper was performed in part in the Environmental Molecular Sciences Laboratory, a national scientific user facility sponsored by the US Department of Energy's Office of Biological and Environmental Research and located at Pacific Northwest National Laboratory in Richland, WA. Pacific Northwest National Laboratory is a multiprogram national laboratory operated for the Department of Energy by Battelle Memorial Institute under Contract DE-AC06-76RLO 1830.

References and Notes

(1) Volcani, B. E. In *Silicon and Siliceous Structures in Biological Systems*; Simpson, T. L., Vocani, B. E., Eds.; Springer: New York, 1981; p 157.

(2) Schraer, R. In *Biological Calcification: Cellular and Molecular Aspects*; Schraer, H., Ed.; Appleton-Century-Crofts: New York, 1970; p 247.

(3) Fritz, M.; Bechler, A. M.; Radmacher, M.; Walters, D. A.; Hansma, P. K.; Stucky, G. D.; Morse, D. E *Nature* **1994**, *371*, 49.

(4) Sarikaya, M.; Aksay, I. A. *Biomimetics: Design and Processing of Materials*; AIP Press: New York, 1995.

(5) Mann, S. *Biomimetic Materials Chemistry*; VCH: Weinheim, Germany, 1996.

(6) Davis, S. A.; Breulmann, M.; Rhodes, K. H.; Zhang, B.; Mann, S. *Chem. Mater.* **2001**, *13*, 3218.

(7) Ogasawara, W.; Shenton, W.; Davis, S. A.; Mann, S. *Chem. Mater.* **2000**, *12*, 2835.

(8) Meldrum, F. C.; Seshadri, R. *Chem. Commun.* **2000**, 29.

(9) Chia, S.; Urano, J.; Tamanoi, F.; Dunn, B.; Zink, J. I. *J. Am. Chem. Soc.* **2000**, *122*, 6488.

(10) Anderson, M. W.; Holmes, S. M.; Hanif, N.; Cundy, C. S. *Angew. Chem., Int. Ed.* **2000**, *39*, 2707.

(11) Shenton, W.; Pum, D.; Sleytr, U. B.; Mann, S. *Nature* **1997**, *389*, 585.

(12) Zhang, B.; Davis, S. A.; Mendelson, N. H.; Mann, S. *Chem. Commun.* **2000**, 781.
(13) Fowler, C. E.; Shenton, W.; Stubbs, G.; Mann, S. *Adv. Mater.* **2001**, *13*, 1266.
(14) Greil, P.; Lifka, T.; Kaindl, A.; *J. Eur. Ceram. Soc.* **1998**, *18*, 1961
(15) Greil, P. *J. Eur. Ceram. Soc.* **2001**, *21*, 105.
(16) Ota, T.; Imaeda, M.; Takase, H.; Kobayashi, M.; Kinoshita, N.; Hirashiata, T.; Miyazaki, H.; Hikichi, Y. *J. Am. Ceram. Soc.* **2000**, *83*, 1521.
(17) Dong, A.; Wang, Y.; Tang, Y.; Ren, N.; Zhang, Y.; Yue, Y.; Gao, Z. *Adv. Mater.* **2002**, *14*, 926.
(18) Shin, Y.; Liu, J.; Zhang, J. H.; Nie, Z.; Exarhos, G. J. *Adv. Mater.* **2001**, *13*, 728.
(19) Ito, T.; Fraissard, J. *J. Chem. Phys.* **1982**, *76*, 5225.
(20) Ripmeester, J. A. *J. Am. Chem. Soc.* **1982**, *104*, 289.
(21) Barrie, P. J.; Klinowski, J. *Prog. NMR Spectrosc.* **1992**, *24*, 91.
(22) Raftery, D.; Chmelka B. F. *NMR Basic Princ. Prog.* **1994,** *30*, 111.
(23) Ratcliffe, C. I. *Annu. Rep. NMR Spectrosc.* **1998**, *36*, 124.
(24) Moudrakovski, I. L.; Terskikh, V. V.; Ratcliffe, C. I.; Ripmeester, J. A.; Wang, L.-Q.; Shin, Y.; Exarhos, G. J.; *J. Phys. Chem. B* **2002**, *106* (23), 5938.
(25) (a)Grover, B. C. *Phys. Rev. Lett.* **1978**, *40*, 391. (b) Happer, W., Miron, E.; Schaefer, S.; Schreiber, D.; van Wingaarden, W. A.; Zeng, X. *Phys. Rev. A* **1984**, *29*, 3092. (c) Driehuys, B.; Cates, G. D.; Miron, E.; Sauer, K.; Walter, D. K.; Happer, W. *Appl. Phys. Lett.* **1996**, *69*, 1668.
(26) Beck, J. S.; Vartuli, J. C.; Roth, W. J.; Leonowicz, M. E.; Kresge, C. T.; Schmitt, K. D.; Chu, C. T.-W.; Olson, D. H.; Sheppard, E. W.; McCullen, S. B.; Hihhins, J. B.; Schlenker, J. L. *J. Am. Chem. Soc.* **1992**, *114*, 10834.
(27) Huo, Q.; Margolese, D. I.; Ciesla, U.; Feng, P.; Gier, T. E.; Sieger, P.; Leon, R.; Petroff, P. M.; Schuth, F.; Stucky. G. D. *Nature* **1994**, *368*, 317. Huo, Q.; Margolese, D. I.; Ciesla, U.; Demuth, D. G.; Feng, P.; Gier, T. E.; Sieger, P.; Chmelka, B. F.; Stucky. G. D. *Chem. Mater.* **1994**, *6*, 1176.
(28) Huo, Q.; Margolese, D.; Stucky, G. D. *Chem. Mater.* **1996**, *8*, 1147.
(29) Christiansen, S. C.; Zhao, D.; Janicke, M. T.; Landry, C. C.; Stucky, G. D.; Chmelka, B. F. *J. Am. Chem. Soc.* **2001**, *123*, 4519.
(30) Kolodziejski, W.; Corma, A.; Navarro, M. T. Pariente, J. *Solid-State NMR* **1993**, *2*, 253.
(31) Steel, A.; Carr, S. W.; Anderson, M. W. *Chem. Mater.* **1995**, *7*, 1829.
(32) Wang, L.-Q, Liu, J.; Exarhos, G. J.; Bunker, B. C. *Langmuir* **1996**, *12*, 2663.
(33) Clauss, J.; Schmidt-Rohr, K.; Adam, A.; Boeffel, C.; Spiess, H. W. *Macromolecules* **1992**, *25*, 5208.
(34) Schmidt-Rohr, K.; Clauss, J.; Spiess, H. W. *Macromolecules* **1992**, *25*, 3273.
(35) Moudrakovski, I.; Lang, S.; Ratcliffe, C. I.; Simard, B.; Santyr, G.; Ripmeester, J. *J. Magn. Res.* **2000**, *144*, 372.
(36) Dixon, W. T. *J. Chem. Phys.* **1982**, *77*, 1800.
(37) (a) Terskikh, V.; Mudrakovski, I.; Mastikhin, V. *J. Chem. Soc. Faraday Trans.* **1993**, *89*, 4239. (b) Terskikh, V. V.; Moudrakovski, I. L.; Breeze, S. R.; Lang, S.; Ratcliffe, C. I.; Ripmeester, J. A.; Sayari, A. *Langmuir* **2002**, *18*, 5653.
(38) Atalla, R. H.; Gast, J. C.; Sindorf, D. W.; Bartuska, V. J.; Maciel, G. E.; *J. Am. Chem. Soc.* **1980**, *102*, 3249.
(39) Lewis, N. G.; Razal, R. A.; Dhara, K. P.; Tamamoto, E.; Bokelman, G. H.; Wooten, J. B. *J. Chem. Soc. Chem. Commun.* **1988**, 1626.
(40) Maunu, S. L. *Prog. NMR Spectrosc.* **2002**, *40*, 151.
(41) Engelhardt, G.; Michel, D. *High-Resolution Solid-State NMR of Silicates and Zeolites*; John Wiley & Sons: New York, 1987.
(42) Brinker, C. J.; Scherer, G. W. *Sol−Gel Science: The Physics and Chemistry of Sol−Gel Processing*; Academic Press: San Diego, CA, 1990.
(43) Glasser, W. G.; Sarkanen, S. *Lignin: Properties and Materials* ACS Symposium Series 397; American Chemical Society: Washington, DC, 1989.
(44) Scurfield, G.; Segnit, E. R. *Sediment. Geol.* **1984**, *39*, 149.
(45) Drum, R. W. *Science* **1968**, *161*, 175.
(46) Ota, T.; Takahashi, M.; Hibi, T.; Ozawa, M.; Suzuki, S.; Hikichi, Y.; *J. Am. Ceram. Soc.* **1995**, *78*, 3409.